Laser Manipulation of Helium: The Limits of the Semi-Classical Description.

A. Aspect, O. Emile, C. Gerz, R. Kaiser, N. Vansteenkiste
H. Wallis (*) and C. Cohen-Tannoudji

Collège de France
et Laboratoire de Spectroscopie Hertzienne de l'Ecole Normale Supérieure
Associé au CNRS et à l'Université Pierre et Marie Curie
24 rue Lhomond, F75005 Paris, France

1. – Introduction.

When one wants to describe the mechanical effects of light on an atom, the most natural approach is the so-called semi-classical treatment [1]. The atom is treated as a pointlike object with a classical trajectory, so that we can use the classical notions of position and of velocity: the effect of light can thus be described by a force, which can be decomposed in a constant part (average force) and a fluctuating part (Langevin force). In order to calculate this force, one must describe the atom-light interaction within the framework of quantum mechanics: first, the internal degrees of freedom of the atom are quantized; second, the quantization of light also plays an essential role (even if a classical description of the laser beam is used), since it is responsible for the fluctuations of the radiative force around its mean value, through the randomness occurring in the absorption and the emission of photons.

In order to evaluate the validity of the semi-classical treatment, one can start from a full quantum treatment, in which the atomic motion is described by a statistical mixture of wave packets [1]. The complete description thus relies on a density matrix involving internal and external degrees of freedom of the atom. The semi-classical description of the first paragraph can be considered as an approximation of the full quantum treatment, valid only if the atomic wave packets are well localized both in real space and in momentum space. The sharp

(*) Permanent address: Institut für Angewandte Physik der Universität Bonn, Wegelerstrasse 8, D5300 Bonn 1, Federal Republic of Germany.

localization in space requires the coherence length L_c of the wave packets to be small compared to the wavelength λ_L of the light. Using the relation $L_c = \hbar/\delta p$, where δp is the width of the atomic-momentum distribution, we obtain a first condition:

$$\delta p > \hbar k_L \,, \tag{1}$$

where we have introduced *the one-photon recoil momentum* $\hbar k_L$ (*i.e.* the atomic-momentum change when the atom absorbs or emits one photon). The second condition (localization in the momentum space) states that the variation of the Doppler effect over the momentum width of the wave packet is small compared to the damping rate Γ of the internal degrees of freedom of the atom (Γ is the natural linewidth in the case of a two-level atom). This condition reads:

$$\delta p < M\Gamma/k \,. \tag{2}$$

These two conditions can be simultaneously fulfilled, provided that the one-photon recoil energy $(\hbar k_L)^2/2M$ be small compared to $\hbar\Gamma$. In that case, the first-order expansion of the full quantum treatment allows one to derive a partial differential equation for the atomic-momentum distribution (Fokker-Planck equation) [2], whose coefficients can be interpreted as an average radiative force and a momentum diffusion coefficient related to fluctuations of the radiative force.

When the average force and the momentum diffusion coefficient can be directly calculated [1], the semi-classical treatment above is very fruitful. For instance, the result of the so-called Doppler cooling, or of laser cooling by polarization gradients, may be studied by finding the steady-state solution of the Fokker-Planck equation [3, 4]. The validity of the semi-classical approach can be checked by verifying that the corresponding momentum distribution obeys conditions (1) and (2).

However, it is possible to achieve very efficient cooling, yielding a momentum distribution with a width close to the one-photon recoil [5], or even below [6], and condition (1) is no longer fulfilled. In such cases, a full quantum description is required. The evolution of the density matrix describing the atoms is then determined by the so-called generalized optical Bloch equations [7], which are a set of first-order differential equations relative to time, quite easy to solve numerically step by step (the main difficulty is the size of the density matrix which may be quite large). One then obtains the time evolution of the momentum distribution. This method has been applied successfully to the cooling below the one-photon recoil [6], or to polarization gradient cooling [8].

In this seminar, we would like to point out other situations in which the use of generalized optical Bloch equations may be preferred to a semi-classical treatment, even though conditions (1) and (2) are satisfied. First, in order to calculate the momentum distribution with an accuracy better than the one-photon recoil $\hbar k_L$, the Fokker-Planck equation—which results from an expansion as

a function of $\hbar k_L/p$—is not a good enough approximation. This situation precisely happens in the case of metastable helium interacting with a laser at $\lambda_L = 1.083\ \mu m$ on the transition $2\,^3S_1$-$2\,^3P_{0,1,2}$: the one-photon recoil velocity is as large as $9.2\ cm\ s^{-1}$, and it is possible to measure the atomic velocities with a quite better accuracy. In sect. 2, we present experimental results on the *mechanical Hanle effect* observed on the $2\,^3S_1$-$2\,^3P_1$ transition of He*. These results can be completely understood only by taking into account the finite value of the one-photon recoil, which is done naturally in the quantum approach.

Surprisingly, in the situation of sect. 2, it turns out that the quantum treatment is not only more accurate but also simpler than the semi-classical treatment! As a matter of fact, the quantum solution only requires a numerical integration, step by step, of a set of ordinary first-order differential equations. This treatment is specially well suited to the description of the transient regime, which corresponds to our experimental situation where the steady-state regime is not reached. On the other hand, the complete semi-classical treatment requires the average force and the momentum diffusion coefficient to be calculated as a function of the momentum. These values are then introduced into the Fokker-Planck equation, which is not easy to solve numerically, particularly in the transient regime, since it is a partial differential equation. This semi-classical procedure is more complicated than solving the generalized optical Bloch equations.

In sect. 3, we will present another effect observed on the $2\,^3S_1$-$2\,^3P_1$ transition of He*: *magnetically assisted Sisyphus effect*. This effect is a new example of the «Sisyphus type» [3, 4] radiative forces which can be observed when the multilevel structure of the ground state plays a role, because of optical pumping between the differently light-shifted ground sublevels. An originality of the magnetically assisted Sisyphus effect is that the Sisyphus force exhibits a behaviour opposed to the behaviour of the standard resonant radiation pressure, which continues to play a role at large velocities: the net result is a bistability in the momentum space, and the corresponding bimodal momentum distribution has been observed. The study of this effect will again allow us to discuss the semi-classical description *vs.* a full quantum treatment based on the generalized optical Bloch equations.

2. – Mechanical Hanle effect.

2·1. *Simple presentation of the effect.* – We consider an atomic beam, propagating along the ***Ox*** axis, and irradiated at right angle by a resonant laser beam propagating along ***Oz*** (fig. 1). In such a situation, one expects a deflection of the atomic beam due to the resonant radiation pressure from the laser (absorption of laser photons, each changing the atomic linear momentum by $\hbar k_L$, and followed by a spontaneous emission that does not change the atomic momentum on

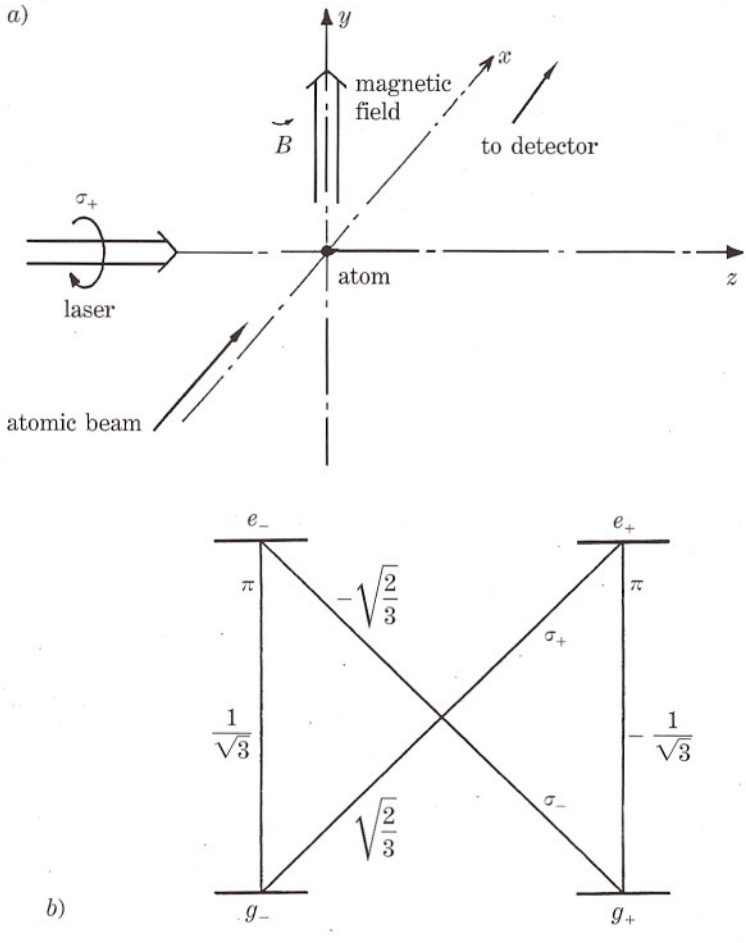

Fig. 1. – Configuration for observing the mechanical Hanle effect. *a*) Experimental configuration: the laser beam is applied transversely to the atomic beam, and can deflect the atoms. This deflection exhibits a resonant variation when the transverse magnetic field is scanned: it is minimum at zero magnetic field. *b*) Simplest atomic-level scheme for observation of the effect: at zero magnetic field, the atoms are optically pumped by the σ_+ circular polarization into g_+, where they no longer interact with the laser, so that there is no deflection. We have indicated the Clebsch-Gordan coefficients characterizing the strength of the transitions.

the average). However, if the laser is σ_+ circularly polarized, and the atomic transition is a $J_g = J \to J_e = J$ transition with the angular momentum J different from zero, the atom is readily pumped into the ground sublevel g_+ associated to the largest value of the angular-momentum component ($m_J = J$), where it no longer interacts with the laser: there is no deflection.

If now we apply a magnetic field $\boldsymbol{B}$ along the third axis $\boldsymbol{Oy}$, there is a Lar-

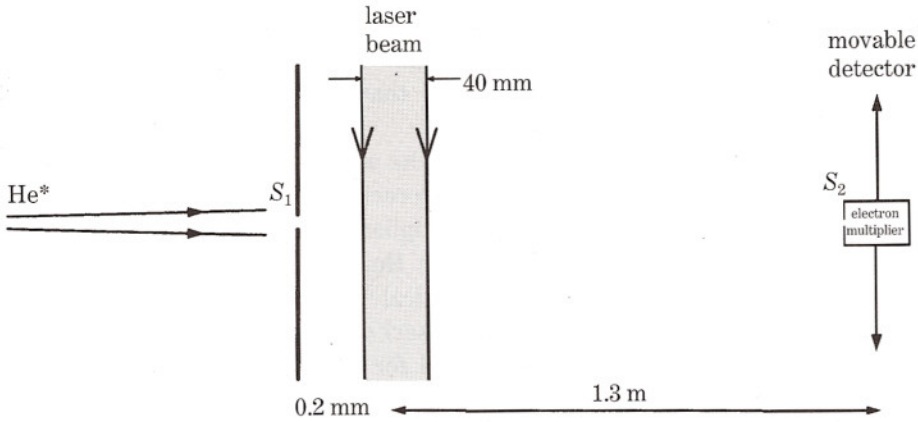

Fig. 2. – Experimental setup. A supersonic beam of metastable helium with a well-defined longitudinal velocity (1100 ms^{-1}), transversely limited by the slit S_1 (0.2 mm wide), is scanned by an electron multiplier with a similar width. This yields the transverse velocity profile. When the laser beam is applied, the beam is deflected, and the modification of the transverse velocity profile is studied.

mor precession in the ground state between g_+ and the other ground sublevels, from which absorption can resume, giving rise to a deflection. If we scan the transverse magnetic field around zero, we thus expect to observe a deflection exhibiting a minimum at zero magnetic field. An order of magnitude of the width of the dip around zero is readily obtained by noticing that the deflection decreases when the Larmor frequency Ω_B becomes small compared to the opti-

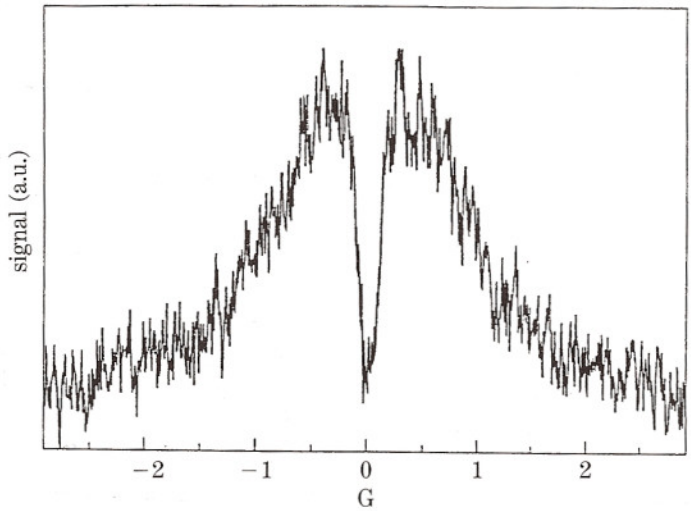

Fig. 3. – Direct detection of the mechanical Hanle effect: signal obtained with the detector fixed in the far wing (opposed to the laser) of the atomic-beam profile. This signal reflects the deflection.

cal pumping rate Γ_p from g_- to g_+. This width may be much narrower than the natural width of the transition, and this signal has all the features of the usual Hanle effect in the ground state [9], except that it is detected by a mechanical effect rather than by optical means.

This effect has been observed [10] with the setup sketched in fig. 2, using an atomic beam of 2^3S_1 metastable helium interacting on the 2^3S_1-2^3P_1 transition with a laser at 1.083 μm. An electron multiplier sensitive to He* can scan the transverse profile of the beam, and it can thus detect a deflection. Figure 3 shows a direct observation of the mechanical Hanle effect, with the detector fixed in the far wing (*i.e.* opposed to the laser) of the atomic-beam profile. Such experiments have proven to be very useful for zeroing with a good sensitivity the magnetic field applied to the atoms [6].

2·2. *Semi-classical calculation.* – We now give the great lines of the semi-classical calculation that we have performed in order to render a quantitative account of the experiment. Within the framework of this approximation, the mean radiative force can be written

$$\boldsymbol{F} = -\langle \boldsymbol{\nabla} V_{AL} \rangle , \tag{3}$$

where

$$V_{AL} = -\boldsymbol{d} \cdot \boldsymbol{E}_L \tag{4}$$

is the electric-dipole interaction Hamiltonian describing the coupling between the atomic dipole moment $\boldsymbol{d}$ and the laser electric field $\boldsymbol{E}_L$ treated as a c-number external field evaluated at the atomic position $\boldsymbol{r}$. In this approach, the atom is considered as a point, and the quantum average appearing in (3) involves only the internal degrees of freedom, so that $\boldsymbol{F}$ can be expressed as a function of the density matrix σ describing the internal atomic state. In order to calculate σ, we use the optical Bloch equations, which describe the evolution of the internal degrees of freedom, taking into account the Hamiltonian interaction with the external magnetic and laser fields, and the damping due to spontaneous emission.

In the so-called rotating-wave approximation, these equations can be written as a set of coupled linear first-order differential equations, with constant (time independent) coefficients, provided that the Doppler effect associated with the velocity change during the interaction remains small compared to the natural width Γ of the transition. The interaction time T is usually long compared to the internal damping time Γ_p^{-1}, and the atoms rapidly reach a steady state: it is thus possible to only look for the steady-state solution of the optical Bloch equations, which is quite simple since it only requires the resolution of a set of linear equations. The results are used to calculate the average force, with formula (3).

A detailed calculation of this type has been presented in ref. [10], in the case

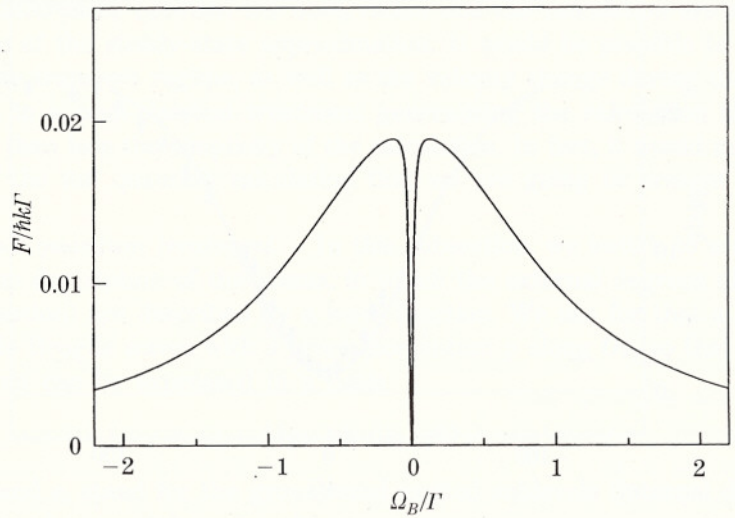

Fig. 4. – This curve presents the result of the semi-classical calculation of the average force exerted by the laser on the atom, in the situation of fig. 1. Ω_B is the Larmor frequency associated to the transverse magnetic field; $\Omega_L = 0.2\Gamma$ is the Rabi frequency associated to the atom-laser coupling; Γ is the natural linewidth of the transition; $\delta = 0$. The mechanical Hanle effect is characterized by the narrow dip around the null value of the magnetic field. The width of this dip, narrower than the natural linewidth Γ, is of the order of the optical-pumping rate Γ_p from g_- to g_+.

of a $J_g = 1/2 \rightarrow J_e = 1/2$ transition. The result is shown in fig. 4, and we see that the average force exhibits a behaviour qualitatively similar to the measurement presented in fig. 3.

2·3. *Quantitative comparison with experiments.* – It must be realized that a completely quantitative interpretation of the experimental results of fig. 3 would require a much more complicated calculation. Indeed, these results reflect the evolution of the momentum distribution, which depends not only on the average force but also on the fluctuations of the force. As indicated in the introduction, this requires the calculation of the momentum diffusion coefficient, and the integration of a Fokker-Planck equation.

In order to be able to compare the experiment to a simpler calculation, we have measured, for each value of the magnetic field, the change Δp of the average transverse atomic momentum: it is easy to show that this quantity is independent of the momentum diffusion coefficient, and that it is related to the average force by the simple equation

$$\Delta p = FT \tag{5}$$

(T is the interaction time between the atoms and the laser). We have plotted in fig. 5 both the experimental and the calculated value of Δp (the calculation, rep-

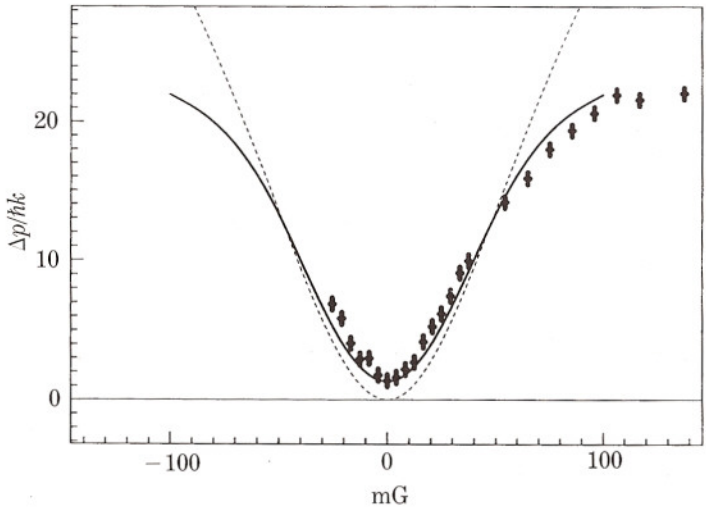

Fig. 5. – Average transverse-momentum change of the atomic beam as a function of the magnetic field. The experimental points are obtained by averaging the profiles obtained with the scanning detector, with and without the laser. The dashed curve is the prediction of the semi-classical treatment of subsect. 2·2. The full curve is the theoretical prediction of the full quantum treatment (subsect. 2·4), where the internal and the external degrees of freedom are quantized: it renders a good account of the transient regime (change of 1.3 $\hbar k_L$ at zero magnetic field) and of the shape of the wings at large magnetic field. $\Omega_L = \Gamma$.

resented by the dotted line, has been done for a $J_g = 1 \rightarrow J_e = 1$ transition, corresponding to the experiment). Although there is reasonable agreement, we clearly see two differences, at large values of the magnetic field and around the null magnetic field.

The difference at large magnetic field happens when the transverse-momentum change is larger than $15\hbar k_L$, *i.e.* when the Doppler effect associated to this momentum change is not negligible compared to the natural linewidth of the transition of metastable helium used in this experiment (1.6 MHz). We know that the calculation above, which uses the steady-state solution at constant velocity, is not valid in this situation.

At zero magnetic field, we attribute the difference to the transient regime, which has been ignored in the calculation. The calculated force is zero, because in the steady state all the atoms are pumped into the ground magnetic sublevel $m_J = 1$, where they no longer interact with the circularly polarized laser. But, in fact, we start with a statistical mixture with equal populations in the three ground-state sublevels, and it requires some fluorescence cycles for all the atoms be pumped into the $m_J = 1$ ground sublevel. A straightforward calculation shows that the average number of cycles per atom is 4/3, which corresponds exactly to the observed momentum change $\Delta p = 1.3\hbar k_L$.

Both differences between the observation and the calculation are related to the failure of the steady-state approximation. It would be possible to take into account the transient regime, as well as the velocity change during the interaction time, in a semi-classical treatment generalizing the calculation above, but we would then lose the simplicity of the calculation. In fact, it would not be simpler than the full quantum calculation that we are going to present now.

2·4. *Full quantum treatment.* – In this subsection, we switch to a completely quantum description of the atoms, in which the external degrees of freedom (*i.e.* the motion) are described by a wave function. We use for that a basis $|p\rangle$ of plane de Broglie waves with a given momentum p along ***Oz***, so that the state of the atom can be expressed in a basis

$$\{|g_i, p\rangle;\ |e_i, p\rangle\}, \tag{6}$$

where g_i and e_i stand for the ground and excited sublevels (internal degrees of freedom), and p can take any value.

In this problem, a remarkable simplification happens: because of the selection rules corresponding to the conservation of angular momentum and of linear momentum, the interaction of the atom with the laser and the magnetic field can only couple a finite number of states (fig. 6). As in ref. [6], we can thus introduce families of states which are closed under the effect of the magnetic field and of absorption and stimulated emission. A family is completely characterized

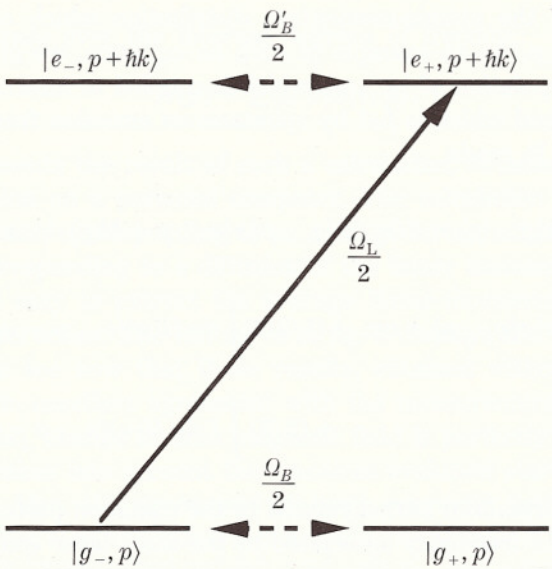

Fig. 6. – Family of states coupled by the laser and the magnetic field, for a $J_g = 1/2 \rightarrow$ $\rightarrow J_e = 1/2$ transition. Because of the conservation of linear momentum, and of angular momentum, the family is closed, *i.e.* there is no other state coupled to this family by the laser or the magnetic field.

by a single value of p. In the case of the $J_g = 1/2 \rightarrow J_e = 1/2$ transition, a family is

$$\mathcal{F}(p) = \{|g_-, p\rangle;\ |g_+, p\rangle;\ |e_-, p + \hbar k_L\rangle;\ |e_+, p + \hbar k_L\rangle\}. \tag{7}$$

If now we consider *intrafamily* density matrix elements, *i.e.* terms of the form

$$\langle \alpha, p|\sigma|\beta, p'\rangle, \tag{8}$$

where $|\alpha, p\rangle$ and $|\beta, p'\rangle$ belong to the *same family*, they are only coupled to *intrafamily* elements of the same family by the interaction of the atom with the laser and the magnetic field.

Spontaneous emission allows the atoms to jump between different families: an atom in the state $|e_i, p + \hbar k_L\rangle$ in the family $\mathcal{F}(p)$ can emit a photon with a linear momentum u along Oz ($-\hbar k_L \leqslant u \leqslant \hbar k_L$), and arrive into the state $|g_j, p + \hbar k_L - u\rangle$ in the family $\mathcal{F}(p + \hbar k_L - u)$. However, spontaneous emission can only couple *intrafamily* terms of a family to *intrafamily* terms of another family, and not to *interfamily* terms, *i.e.* terms between two *different families*.

Finally, the evolution equations (generalized optical Bloch equations) couple internal terms of a family to other internal terms of the same family or of other families. We can restrict our study to this type of terms, since our final goal is the calculation of the atomic-momentum distribution which only depends on terms diagonal in p. As an example of such an equation, we give the evolution equation of the population of $|g_-, p\rangle$, which is coupled to internal coherences of the same family, and which is fed by spontaneous emission from excited states of other families. It reads

$$\begin{aligned}\frac{\mathrm{d}}{\mathrm{d}t}\langle g_-, p|\sigma|g_-, p\rangle &= i(\Omega_L/2)\langle g_-, p|\sigma|e_+, p + \hbar k_L\rangle + \text{c.c.} + \\ &+ i(\Omega_B/2)\langle g_+, p|\sigma|g_-, p\rangle + \text{c.c.} + (1/3)\Gamma \int \mathrm{d}u\, H(u)\langle e_+, p - u|\sigma|e_+, p - u\rangle + \\ &+ (2/3)\int \Gamma \mathrm{d}u\, H(u)\langle e_-, p - u|\sigma|e_-, p - u\rangle,\end{aligned} \tag{9}$$

where $H(u)$ is a normalized kernel related to the radiation pattern of the transition, Ω_L is the Rabi frequency associated to the atom-laser coupling, and Ω_B is the frequency associated to the Larmor precession in the ground state.

We thus have a set of first-order differential equations, which can be numerically integrated step by step, after discretization and truncation in p, yielding the density matrix evolution. The atomic-linear-momentum distribution is then

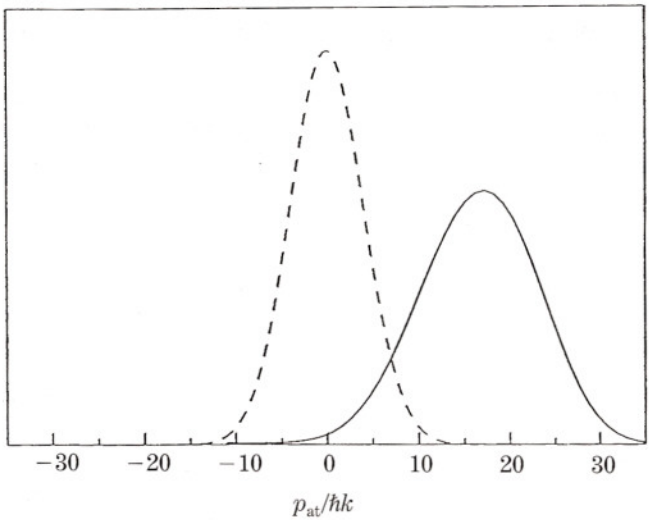

Fig. 7. – Full quantum calculation of the evolution of the atomic-momentum distribution, in the situation of fig. 1. The discontinuous curve is the initial distribution, while the full line represents the distribution after an interaction time of $300\Gamma^{-1}$. The average displacement corresponds to the semi-classical average force. The spread of the distribution corresponds to the fluctuations of the semi-classical force, expressed by a coefficient of diffusion of the momentum. This calculation also renders an account of the transient regime. $B = 50$ mG, $\delta_L = 0$, $\Omega_L = 0.7\,\Gamma$, $\theta_{int} = 300\,\Gamma^{-1}$.

obtained by a trace over the internal degrees of freedom:

$$N(p) = \sum_i \langle i, p | \sigma | i, p \rangle . \tag{10}$$

Figure 7 presents the result of such a calculation, obtained after a few seconds of calculation on a personal computer. The calculation not only shows a global displacement, corresponding to an average force, but also a spread of the distribution, corresponding to a diffusion of the linear momentum. From such a calculation, it is easy to extract the average linear-momentum change after a given time of interaction. The full curve of fig. 5 displays the results of this calculation, and we see now that these results, obtained without any adjustable parameter, are in excellent agreement with the measurement. Note in particular that the $1.3\hbar k_L$ change at zero magnetic field is perfectly reproduced, since our calculation takes into account the transient evolution starting from the real initial situation. Also, the agreement at large magnetic field reflects the fact that our calculation correctly takes into account the change of the Doppler effect when the atom is deflected.

We thus find that the full quantum treatment gives results in excellent agreement with the experimental data, including features (diffusion, transient effects) which would require complicated calculations in the framework of the

semi-classical approach. The quantum calculation is specially simple in this case, because of the existence of the closed families. For this problem, the quantum calculation is not only more rigorous than the semi-classical calculation, it is also simpler.

3. – Magnetically assisted Sisyphus effect.

3·1. *Physical idea.* – Let us consider again the situation of fig. 1, but the circularly polarized laser beam is now a standing wave. In the absence of a magnetic field, the ground-state sublevels have their degeneracy removed by the laser wave, which interacts with g_- and produces a light shift, while g_+, which does not interact with the laser, remains unchanged. Since we have a standing wave, the light shift of g_- is modulated in space, maximum at an antinode and null at a node, as shown in fig. 8. If an atom travels in the standing wave, it is optically pumped into g_+, where it experiences no force since the energy of this level is constant.

Suppose now that we apply a weak transverse magnetic field, producing be-

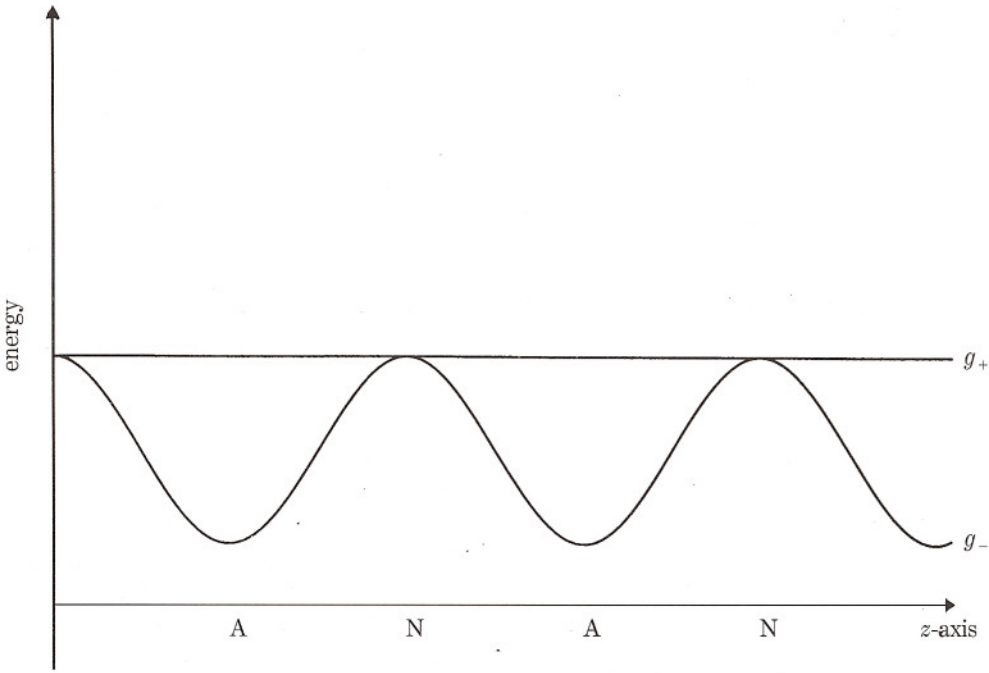

Fig. 8. – Energy values of the ground sublevels for a $J_g = 1/2 \rightarrow J_e = 1/2$ transition excited by a σ_+ circularly polarized standing wave, detuned below resonance. g_-, which is coupled to the light, experiences light shifts null at a node and maximum at an antinode. g_+ is not coupled to the σ_+ polarized light, and it is not light-shifted. Note that optical pumping tends to put the atom in the g_+ sublevel; this is more efficient around the antinodes, where the light intensity is maximum.

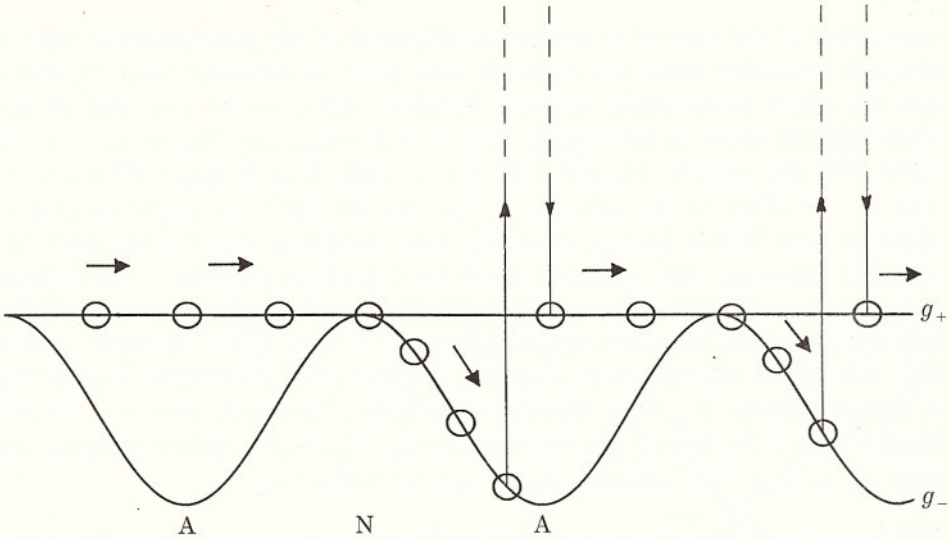

Fig. 9. – Magnetically assisted Sisyphus effect for a $J_g = 1/2 \rightarrow J_e = 1/2$ transition, in the case of a negative detuning. When an atom travels through a node, it experiences a precession because of the transverse magnetic field, and it can leave the nodal region in the g_- sublevel, where it is accelerated, until it is optically pumped to g_+, where it has a uniform motion. The process can resume at the next node, and the net result is an increase of the velocity of the atom.

tween g_- and g_+ a coupling smaller than the value of the light shift at an antinode, so that the levels are almost unchanged at an antinode, and an atom moving around an antinode is still optically pumped into g_+, where it experiences no force. On the opposite, around a node, there is a precession between g_- and g_+, so that an atom travelling through a node may be found in g_- just after the node. On a g_- level, which is modulated, the atom experiences a force: in the case of fig. 8, corresponding to a negative detuning of the laser, the atom is accelerated between the node and the antinode. If the atom remained on the same sublevel, it would then decelerate between the antinode and the following node, and after one period (*i.e.* half a wavelength) the kinetic energy would remain unchanged. In fact, the circularly polarized laser tends to optically pump the atom from g_- to g_+, and this is more likely to happen around the antinode, where the laser intensity is larger. For small velocities such that the usual Doppler cooling plays no role, the kinetic energy does not change (on the average) during the optical-pumping process, and the atom then proceeds on g_+ which is flat. This process is visualized in fig. 9, and we see that the net result is an increase of the kinetic energy of the moving atom. For a positive laser detuning, we would have the opposite conclusion: the kinetic energy of the atom decreases.

The reasoning above is analogous to the one of ref. [3], describing the Sisy-

phus effect in the case of a gradient of ellipticity of the polarization of light. In the case presented here, the magnetic field plays an essential role [11], and we call this effect magnetically assisted Sisyphus effect. As for any kind of Sisyphus effect, it would be possible to show that the corresponding force varies linearly with the velocity around 0. However, there is a striking difference: the sign of our effect is the opposite of the sign in the usual situations [3, 4, 11], since we have here a heating force (the force increases with the velocity) for a negative detuning, and a cooling force for a positive detuning. This different sign has dramatic consequences on the behaviour of the force as a function of velocity, when one does not restrict the study to very small velocities. Indeed, it is well known that Sisyphus cooling is efficient only at velocities smaller than a critical velocity V_s. This velocity is such that the atom travels a distance smaller than a fraction of a wavelength during $(\Gamma_p)^{-1}$ (the optical-pumping time from g_- to g_+). This critical velocity can be defined by

$$V_s = \Gamma_p / k_L \,. \tag{11}$$

When the atomic velocity is larger than V_s, the Sisyphus force vanishes, while the optical-pumping process becomes sensitive to the atomic velocity: because of the Doppler effect, the probabilities of excitation by the two components of the standing wave are no longer equal. The result is the usual Doppler cooling force, which is efficient on a velocity range of the order of V_D, defined by

$$V_D = \Gamma / k_L \tag{12}$$

(note that V_D is larger than V_s). This Doppler force is cooling for a negative detuning, and heating for a positive detuning. The force at large velocities has thus a sign opposed to the Sisyphus force at low velocity (while in the usual cases the two effects have the same sign and just add up).

In order to intuitively understand the physical consequences of this situation, we can add these two forces. First we take the Doppler force in the typical situation of a negative detuning equal to $\Gamma/2$: it is the sum of two opposite Lorentzian curves centred at $-V_D/2$ and $+V_D/2$. We model the Sisyphus force by the expression [8]

$$Fs = \frac{\alpha V}{1 + V^2/V_c^2} \tag{13}$$

with V_c of the order of V_s, *i.e.* smaller than V_D.

Figure 10 shows the result of this addition. The total force vanishes not only at the null velocity, but also at the values V_1 and $-V_1$, so that there are three «equilibrium» points in the velocity space. For a negative detuning (fig. 10), the two points at V_1 and $-V_1$ are stable, while $V = 0$ is unstable (this results from the sign of the slope around each point). If we let an atom ensemble evolve under such a force, we thus expect that the atoms will get bunched around V_1 and $-V_1$, with a velocity distribution exhibiting two bumps, the width of which is

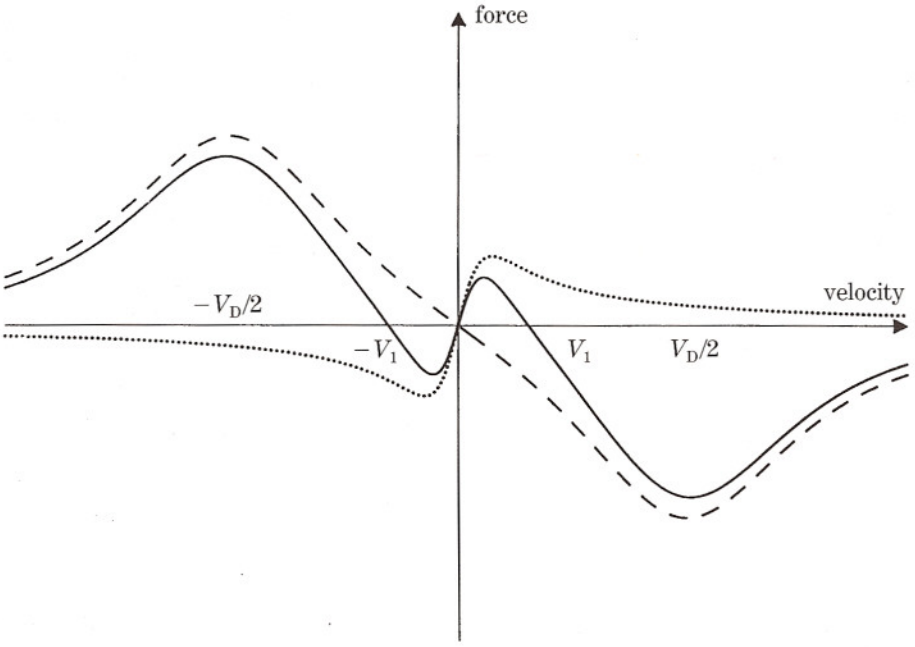

Fig. 10. – Combined effects of the Sisyphus force (dotted curve) and of the Doppler cooling force (discontinuous curve). Since the two effects have opposite signs, and they act on different velocity ranges, the addition results in a curve (full line) crossing the horizontal axis on three points. The two points at $-V_1$ and $+V_1$ are stable-equilibrium points, while zero is unstable.

determined by the unavoidable fluctuations of the force around its average value.

In the case of a positive detuning, we expect a force with the same shape but a reversed sign. The physical consequences are then completely different since we have now only one stable point around $V = 0$, and two unstable points at V_1 and $-V_1$. Atoms initially distributed in the interval $[-V_1, V_1]$ will thus be «attracted» towards $V = 0$, and we expect a final velocity distribution exhibiting a single bump around zero.

Remark. In fact, in the last case, there is no real steady-state distribution since there is a diffusion process in the velocity space, allowing atoms to «jump» above the values V_1 or $-V_1$. However, provided that this escape mechanism has a characteristic time longer than the bunching time, we will be able to observe a «metastable» situation with atoms bunched around $V = 0$.

3·2. *Experiments.* – We have performed some experiments in order to check the validity of the heuristic predictions of subsect. 3·1. The apparatus is the

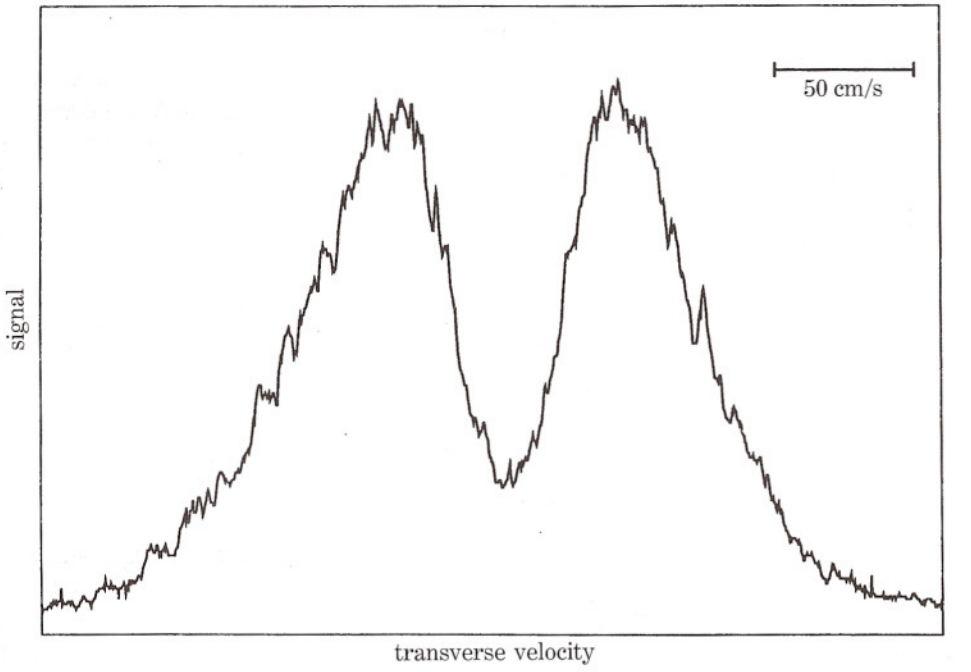

Fig. 11. – Observation of the magnetically assisted Sisyphus effect final for a negative detuning. The final transverse-velocity distribution shows a double bump, corresponding to the two stable points of fig. 10. $\Omega_L = 1.5\,\Gamma$, $\delta = -\Gamma$, $\Omega_B = 0.055\,\Gamma$.

same as the one described in fig. 2, but with a mirror added for retroreflecting the laser beam, to produce a standing wave. Figure 11 presents an example of a doubly-peaked velocity distribution obtained with a negative detuning. This has been obtained with a laser intensity and detuning giving an optical-pumping rate at the antinodes $\Gamma_p = 0.4\Gamma$. The corresponding «Sisyphus velocity» (eq. (11)) is $V_s = 0.6\,\mathrm{ms}^{-1}$. As predicted by our heuristic reasoning, the velocity V_1 of the maximum of the bumps ($0.5\,\mathrm{ms}^{-1}$) is slightly smaller than V_s. The other important experimental parameter is the magnetic field (44 mG). It has been adjusted for giving the best visibility of the bumps, and the corresponding Larmor frequency (0.05Γ) is a fraction of the light shift at the antinodes (0.4Γ). This was expected from the intuitive reasoning of subsect. 3·1.

We have also studied the case of a positive detuning. As shown in fig. 12, it is possible to obtain a bump around zero. The large background reflects the initial velocity distribution, which has not yet been washed out because the interaction time is not long enough ($300\Gamma^{-1}$). A result such as fig. 12 is obtained only if the initial velocity distribution is centred around zero. This confirms that only the atoms which are initially in the interval $[-V_1, V_1]$ can be «attracted» towards $V = 0$.

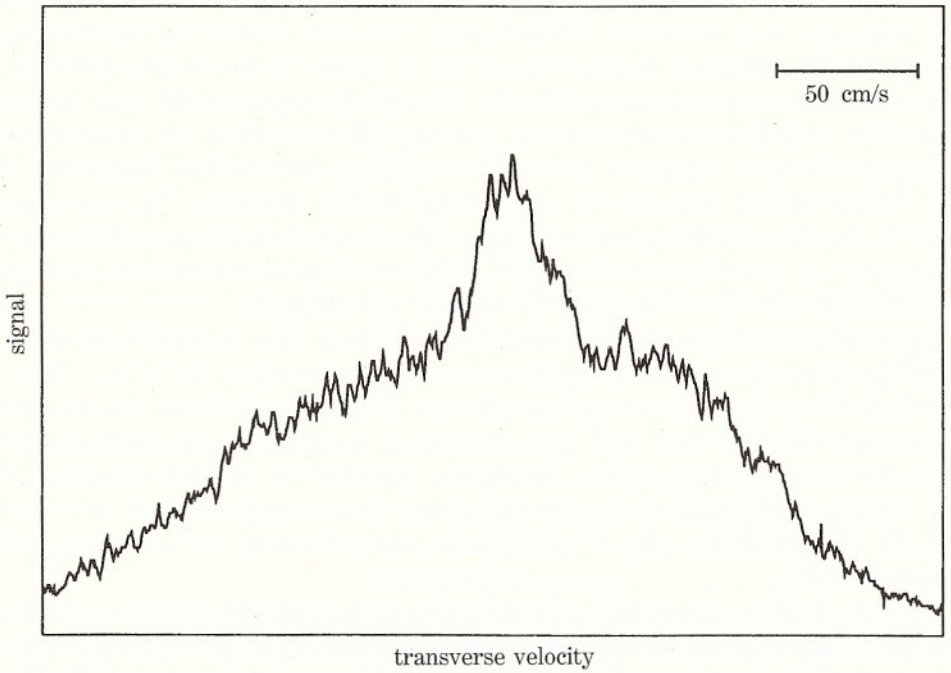

Fig. 12. – Observation of the magnetically assisted Sisyphus effect final for a positive detuning. The final transverse-velocity distribution shows a single bump around the null velocity. The large background reflects the initial velocity distribution which has not yet been washed out at the end of the interaction time ($300\Gamma^{-1}$). $\Omega_L = 1.5\,\Gamma$, $\delta = 4.5\,\Gamma$, $\Omega_B = 0.055\,\Gamma$.

More generally, all the experimental results obtained with various sets of parameters confirm the trends that can be predicted from the intuitive analysis of subsect. 3·1. We have thus tried to give a more quantitative account of the experiments.

3·3. *Semi-classical analysis.* – We now give the great lines of the semi-classical treatment of the magnetically assisted Sisyphus effect, following the same approach as for the mechanical Hanle effect (subsect. 2·2 and ref. [10]). We will thus concentrate on the calculation of the average force exerted by the laser upon the atom, in the steady-state situation corresponding to a constant velocity for the atom.

In order to simplify the reasoning, we suppose that there is no Zeeman effect in the excited state, so that there is no magnetic coupling between e_- and e_+; since there is no coupling between the laser and e_-, we can restrict the system to the 3 levels (g_-, g_+, e_+). There are then 9 optical Bloch equations, describing the evolution of the density matrix for these three levels. Because of

the modulation of the light, the coefficients corresponding to the coupling with the laser are now modulated in time when the atom travels in the standing wave, and the notion of steady state is not as simple as previously. However, for an atom moving at constant velocity, this modulation is periodic, and we can look for a modulated solution with the same period: this will be the steady-state solution. A Fourier expansion allows one to express each Fourier component of the density matrix elements as a continued-fraction expansion [12] depending only on the laser detuning and intensity, on the magnetic field and on the atomic velocity. It is well known that such continued-fraction expansions converge rapidly, and are very well suited to numerical calculations.

In fact, since we are only interested in the average force exerted by the laser standing wave, we only need to know the optical coherence $\langle g_- |\sigma| e_+ \rangle$. More precisely, in order to obtain the constant part of this average force, it is enough to calculate the first term of $\langle g_- |\sigma| e_+ \rangle$, which is modulated as the laser intensity in the standing wave. Such a calculation, repeated for the various values of the velocity, has allowed us to plot the average force as a function of the velocity, for the interesting sets of parameters (laser detuning and intensity, and magnetic field).

Figure 13 shows an example of such a plot, for parameters similar to the experimental ones for fig. 11. We see that the calculated value has a general shape as predicted by the heuristic argument of subsect. 3·1, and displayed in fig. 10. It thus confirms that the appearance of a double bump corresponds to a bistable equilibrium. We can even check that the position of these bumps corresponds roughly to the points $-V_1$ and $+V_1$ where the plot of fig. 13 intersects the zero-force axis with a negative slope.

However, as in the case of the mechanical Hanle effect, a detailed comparison with experimental data obtained in various situations reveals some discrepancies. Here again, these discrepancies can be related to the fact that the knowledge of the steady-state average force does not describe the whole phenomenon. First, the interaction time is not very long compared to the time required for the atoms to bunch around the equilibrium points under the effect of the average force (this required time may be very long for atoms initially at zero velocity). Second, one should take into account the diffusion of the velocity due to fluctuations in the exchange of momentum between the light and the atoms: this diffusion has an effect not only on the transient regime, but also on the shape of the steady-state velocity distribution [13]: for instance, the bump around V_1 may be strongly asymmetric if the slope of the average force is not constant; taking into account the noise in the measurement, this can lead to an apparent shift of the average position of the bump. We thus come again to the conclusion that a precise comparison with the experiment demands that the theory take into account the diffusion and the transient behaviour. Following the previous line, we have rather tried to take these effects into account by resorting to a full quantum description.

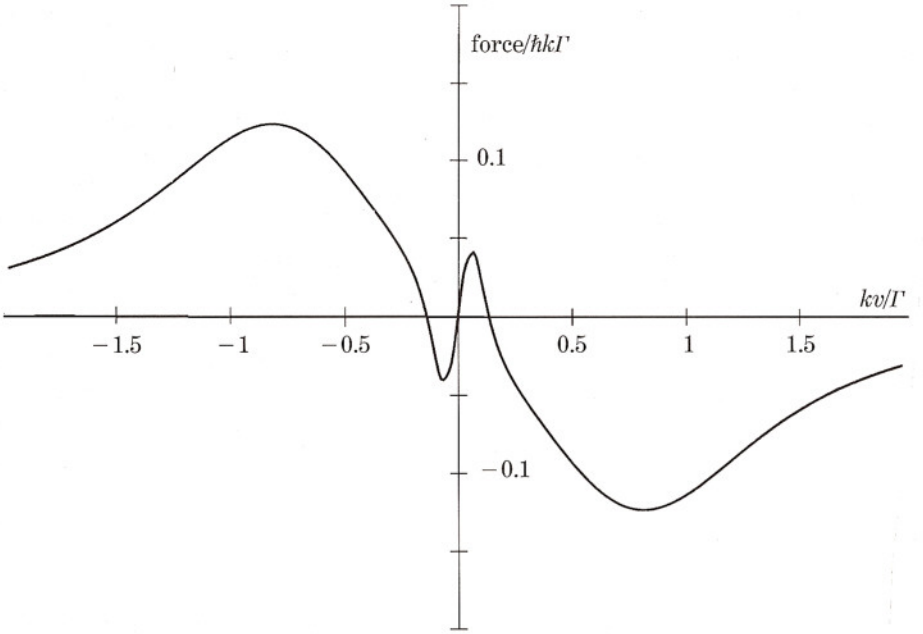

Fig. 13. – Result of the semi-classical calculation of the average force for parameters corresponding to those of fig. 11. This calculation, based on a continued-fraction expansion, has been performed for the $J_g = 1 \rightarrow J_e = 1$ transition of metastable helium used in the experiment. $\delta = -0.5\,\Gamma$, $\Omega_L = \Gamma$, $\Omega_B = 0.055\,\Gamma$.

3·4. *Full quantum treatment.* – We now describe the atomic state in a basis incorporating a quantum number p associated to the quantized linear momentum of the atom. We can then write generalized optical Bloch equations, describing the evolution of the generalized density matrix under the effect of the Hamiltonian and of the spontaneous emission. In the situation considered here, there are no closed families of states, and, as shown in [8], the study bears on a large number of density matrix elements. More precisely, one must study the evolution of terms $\langle i, p' | \sigma | j, p'' \rangle$ with all possible values of momentum for p' and p'', and of internal degrees of freedom for i and j. This makes the numerical resolution of the generalized optical equations somewhat lengthy, because of the large number of such elements. Suppose, for instance, that p is discretized on 40 values, and that we consider the 6 levels of a $J_g = 1 \rightarrow J_e = 1$ transition; there are 57600 such terms, and thus 57600 equations to integrate step by step. This has been done on a work station, and fig. 14 shows a preliminary result. Although our analysis is not yet completed, the checks that we have done confirm that these calculations, which describe accurately the transient regime including diffusion effects, give a better agreement with the experimental data.

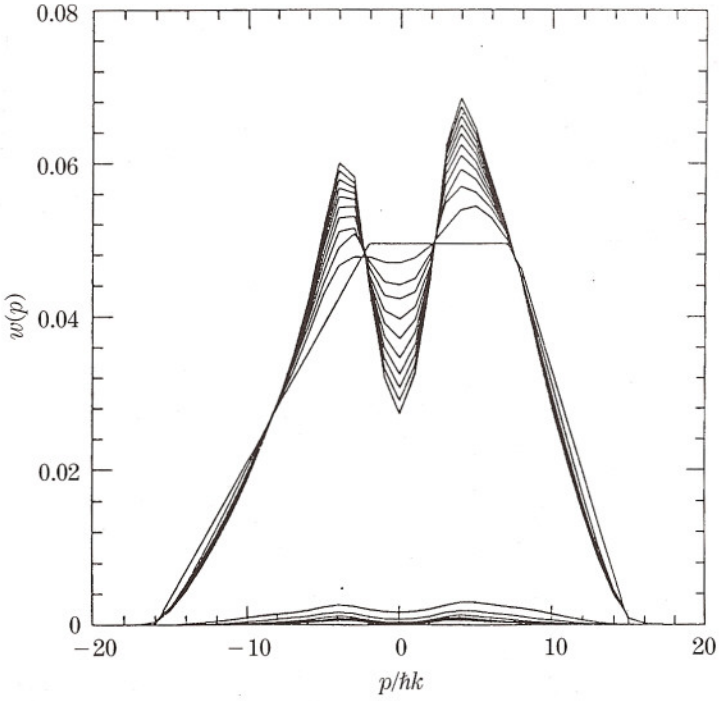

Fig. 14. – Result of a full quantum calculation of MASE for a negative detuning. The initial distribution has been taken asymmetric, and the shape of the velocity distribution during the transient regime strongly depends on this asymmetry. The profiles are plotted every $50\Gamma^{-1}$. $\delta = -1.1\,\Gamma$, $\Omega_L = 2.4\,\Gamma$, $\Omega_B = 0.06\,\Gamma$.

4. – Conclusion.

In this seminar, we have presented two new mechanical effects of a laser on an atom, for a $J_g = J \rightarrow J_e = J$ transition, in the presence of a magnetic field. The *mechanical Hanle effect* is very sensitive to the magnetic field, and it can be used as a test of compensation of stray magnetic fields. The *magnetically assisted Sisyphus effect* has, in this case, the interesting feature to be opposed to the usual Doppler cooling effect, and the atoms have a bistable behaviour in the velocity space.

Both effects can be understood within the framework of a semi-classical treatment, but a precise comparison with the experimental data is not easy to obtain in this framework. On the opposite, we have seen that a full quantum treatment can be derived in a straightforward way, and that the corresponding equations may be quite easy to solve, even though this sometimes demands a large computer memory. Since the full quantum treatment takes automatically into account all the features which are difficult to handle in the semi-classical treatment (fluctuations of the force, transient regime), this treatment may be

preferred when one wants precise calculations, even in the case when the semi-classical treatment is valid in principle.

We would like nevertheless to add a caveat. All the physical ideas and intuitive predictions are easy to present within the framework of the semi-classical picture, where we think of an atom as a pointlike particle interacting with light. It seems much more difficult to get intuitions from a full quantum description of the atom in terms of density matrix including the external degrees of freedom [14]. Our experience is that the semi-classical description can be very useful for finding situations in which interesting effects may appear.

As an example, we can raise the question of the effect of a longitudinal component of the magnetic field in the situation of MASE. A simple inspection of fig. 8 and 9 allows us to find an interesting situation: for a well-chosen longitudinal magnetic field, the ground level g_+ may be shifted to the lowest position of g_-, so that, for a negative detuning, the Sisyphus effect will now cool instead of heating. This dramatic change of behaviour has been observed experimentally, after it had been guessed thanks to the semi-classical description.

* * *

The authors acknowledge many fruitful discussions with J. DALIBARD and CH. SALOMON. This work has been supported by Direction des Recherches et Etudes Techniques.

REFERENCES

[1] R. J. COOK: *Phys. Rev. A*, **20**, 224 (1979); *Phys. Rev. Lett.*, **44**, 976 (1980); J. P. GORDON and A. ASHKIN: *Phys. Rev. A*, **21**, 606 (1980). For a general presentation, see C. COHEN-TANNOUDJI: in *Fundamental Systems in Quantum Optics*, Les Houches Session LIII (Elsevier Science Publisher, Amsterdam, to appear in 1992).

[2] J. DALIBARD and C. COHEN-TANNOUDJI: *J. Phys. B*, **18**, 1661 (1985), and references therein.

[3] J. DALIBARD, C. SALOMON, A. ASPECT, E. ARIMONDO, R. KAISER, N. VANSTEENKISTE and C. COHEN-TANNOUDJI: in *Proceedings of ELICAP (Paris, 1988)*, edited by S. HAROCHE, J. C. GAY and G. GRYNBERG (World Scientific, Singapore, 1989), p. 199: J. DALIBARD and C. COHEN-TANNOUDJI: *J. Opt. Soc. Am. B*, **6**, 2023 (1989).

[4] P. J. UNGAR, D. S. WEISS, E. RIIS and S. CHU: *J. Opt. Soc. Am. B*, **6**, 2058 (1989).

[5] P. LETT, R. WATTS, C. WESTBROOK, W. D. PHILLIPS, P. GOULD and H. METCALF: *Phys. Rev. Lett.*, **61**, 169 (1969); Y. SHEVY, D. S. WEISS, P. J. UNGAR and S. CHU: *Phys. Rev. Lett.*, **62**, 1118 (1969); A. M. STEANE and C. J. FOOT: *Europhys. Lett.*, **14**, 231 (1991); B. SHEEHY, S-Q. SHANG, P. VAN DER STRATEN, S. HATAMIAN and H. METCALF: *Phys. Rev. Lett.*, **64**, 858 (1990); C. MONROE, W. SWANN, H. ROBINSON and C. WIEMAN: *Phys. Rev. Lett.*, **65**, 1571 (1990); C. SALOMON, J. DALIBARD, W. D. PHILLIPS, A. CLAIRON and S. GUELLATI: *Europhys. Lett.*, **12**, 683 (1990).

[6] A. ASPECT, E. ARIMONDO, R. KAISER, N. VANSTEENKISTE and C. COHEN-TANNOUDJI: *Phys. Rev. Lett.*, **61**, 826 (1988); *J. Opt. Soc. Am. B*, **6**, 2112 (1989).

[7] C. BORDÉ: in *Advances in Laser Spectroscopy*, edited by F. T. ARECCHI, F. STRUMIA and H. WALTHER (Plenum Press, New York, N.Y., 1983), p. 1; S. STENHOLM: *Appl. Phys.*, **16**, 159 (1978).

[8] Y. CASTIN, J. DALIBARD and C. COHEN-TANNOUDJI: in *Light Induced Kinetic Effects on Atoms, Ions, and Molecules*, edited by L. MOI, S. GOZZINI, C. GABBANINI, E. ARIMONDO and F. STRUMIA (Ets Editrice, Pisa, 1991), p. 5.

[9] J. C. LEHMAN and C. COHEN-TANNOUDJI: *C. R. Acad. Sci.*, **258**, 4463 (1964).

[10] R. KAISER, N. VANSTEENKISTE, A. ASPECT, E. ARIMONDO and C. COHEN-TANNOUDJI: *Z. Phys. D*, **18**, 17 (1991).

[11] Effects analogous to the magnetic assisted Sisyphus effect described here have already been presented in ref. [4] and in B. SHEEHY *et al.* (ref. [5]). However, these authors had only considered situations ($J_g = J \to J_e = J + 1$ transitions) where the Sisyphus force has the same sign as the usual Doppler force, so that it increases the amount of cooling.

[12] V. G. MINOGIN and O. T. SERIMAA: *Opt. Commun.*, **30**, 373 (1979).

[13] It is well known that a bistable behaviour may be strongly affected by the presence of a fluctuating driving force. See, for instance, G. BROGGI and L. A. LUGIATO: *Phys. Rev. A*, **29**, 2949 (1984); W. LANGE, F. MITSCHKE, R. DESERNO and J. MLYNEK: *Phys. Rev. A*, **32**, 1271 (1985); E. ARIMONDO, D. DANGOISSE and L. FRONZONI: *Europhys. Lett.*, **4**, 287 (1987).

[14] The recently introduced *Wavefunction Monte-Carlo approach* (J. DALIBARD, Y. CASTIN and K. MØLMER: submitted for publication), or *Quantum jumps Monte-Carlo approach* (C. COHEN-TANNOUDJI, F. BARDOU and A. ASPECT: in *Proceedings of Tenicols*, edited by M. DUCLOY, E. GIACOBINO and G. CAMY (World Scientific, Singapore, 1991), p. 3), may constitute a valuable way to develop intuitions in a full quantum framework.